

A FIRST LOOK AT ORBIT DETERMINATION FOR THE CASSINI MISSION

PART 1: INNER SOLAR SYSTEM THROUGH PROBE DELIVERY

Anthony H. Taylor*, Rodica Ionasescu*, and Robin M. Vaughan*

This paper summarizes the first round of orbit determination analysis accomplished as part of navigation studies for the Cassini mission. Thrust of the analysis has been to characterize operational orbit determination accuracy to first order for selected phases of the mission, and as such, the results here are a representative snapshot of a continually evolving state of knowledge of Cassini orbit determination. Results are presented for four phases: the inner solar system flybys of Venus and Earth, the approach to Saturn, the Huygens Probe delivery to Titan, and representative orbits from the Saturn tour. Simulations and a priori assumptions are described, including selection and scheduling of data types, modeling of spacecraft dynamics, and filter configuration. Current estimates of orbit determination accuracy are given along with results of experimentation with various scenarios. Sensitivities to error sources are discussed. This paper is divided into two parts: Part 1 covers the first three phases, from the inner solar system through the Huygens Probe delivery, and Part 2 covers the Saturn Tour.

INTRODUCTION

Accurate orbit determination is an important ingredient for the successful completion of the Cassini mission. The Cassini Orbiter with its Huygens Probe is scheduled for launch in October of 1997 into a trajectory which will carry the combined spacecraft through gravity assist flybys of Venus (twice), Earth, and Jupiter before arrival at Saturn in June of 2001 when it will begin a 4-year tour of the Saturn system (See Figures 1 and 2). During the first orbit around Saturn, the Huygens Probe separates from the Orbiter and enters Titan's atmosphere 21 days later to impact the surface. The Orbiter continues the tour, accomplishing multiple close encounters with Titan. Several encounters with the smaller, icy satellites are also accomplished. Each of the mission phases presents different challenges to the operational orbit determination process of using radiometric tracking and onboard optical data to accurately estimate spacecraft trajectories in the presence of errors. Orbit knowledge is needed for spacecraft safety (e.g., not hitting Titan), efficient use of fuel (large trajectory knowledge errors could result in premature depletion of fuel and consequent end of the mission), prediction of encounter trajectories and uncertainties for science and mission planning, and reconstruction of trajectories and uncertainties for science data reduction.

An initial round of analysis for operational Orbit Determination (OD) has been completed and is summarized here for major phases of the mission. Data covariance analyses using simulated data in programs similar to operational OD software were used to generate orbit uncertainties for representative trajectories in each phase. One of the goals of these analyses was to determine OD capabilities and sensitivities to parameter errors; another was to determine whether less data could be used than currently

* Member Technical Staff, Navigation Systems Section, Jet Propulsion Laboratory, California Institute of Technology, 4800 Oak Grove Drive, Pasadena, CA 91109.

required in order to lower operations costs. Cost reductions could also be realized if requirements for some of the "enhanced" radiometric data types such as *Differenced Doppler* and *NDOR* could be dropped.

In the following sections, assumptions and results are summarized for the inner solar system flybys of Venus and Earth, the approach to Saturn, and the Huygens Probe delivery to Titan. The Saturn orbital tour phase will be covered in a second part of this paper. The only major areas not addressed, because they have not yet been studied, are the Jupiter flyby and the icy satellite encounters.

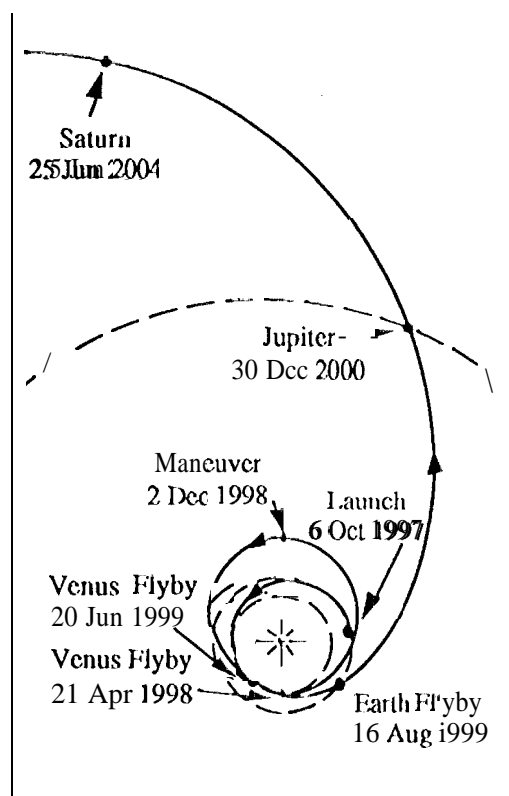


Figure 1 Interplanetary phase from launch until arrival at Saturn.

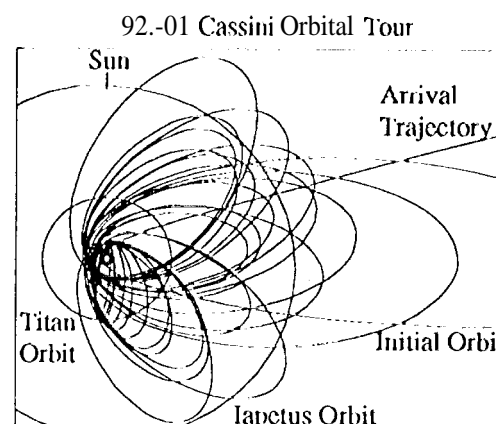


Figure 2 Arrival at Saturn and Cassini Orbital tour.

INNER SOLAR SYSTEM — VENUS AND EARTH FLYBYS

There are currently three launch periods for the Cassini mission, each with different trajectory characteristics for the inner solar system phase. The prime mission launch occurs in October 1997; Cassini then flies a Venus-Venus-Earth-Jupiter Gravity Assist (VVEJGA) trajectory. The secondary launch period, two months later in December 1997, is associated with a VVEJGA trajectory, and the backup launch period in March 1999 is associated with a different VVEJGA trajectory. The OD analysis was done for the prime mission. Analysis for the secondary and backup missions has yet to be undertaken, but most major results from the prime mission can be carried over to the other two.

The thrust of the analysis was to determine the basic OD capability in terms of orbit knowledge at the last trajectory control time before each flyby. Other areas were addressed as well, which included sensitivities both to variations of a priori covariances and reductions of the amount of tracking data. A large uncertainty is undesirable from a fuel usage standpoint because it requires a large maneuver after the flyby to clean up the delivery error. It is also undesirable from a safety standpoint for a close flyby. There is currently no explicit requirement on the size of the OD delivery uncertainty, but for the purpose of the analysis 50 km (1 σ) was used as a standard against which to measure performance. This is the uncertainty which just depletes the navigation AV allocation for the inner solar system phase.

setup

Figure 3 shows the portions of the VVJGA trajectory used in the covariance study. A launch date of 27 October 1997 was chosen from the prime launch period (6 – 30 October 1997). Two independent data arcs, whose trajectories were fixed by this launch date, were started 90 days before the Venus 1 and Venus 2 flybys (Venus 1 occurs about 7 months after the assumed launch date; Venus 2 is about 14 months after Venus 1). The Venus 2 arc leads into the approach to Earth, and so the Earth results were obtained by continuing along the second arc without any reinitialization. The flyby altitudes for this particular trajectory were 4208 km for the Venus 1 prograde flyby, 300 km for the Venus 2 retrograde flyby, and 1204 km for the prograde Earth flyby, but the altitudes vary considerably across the launch period.

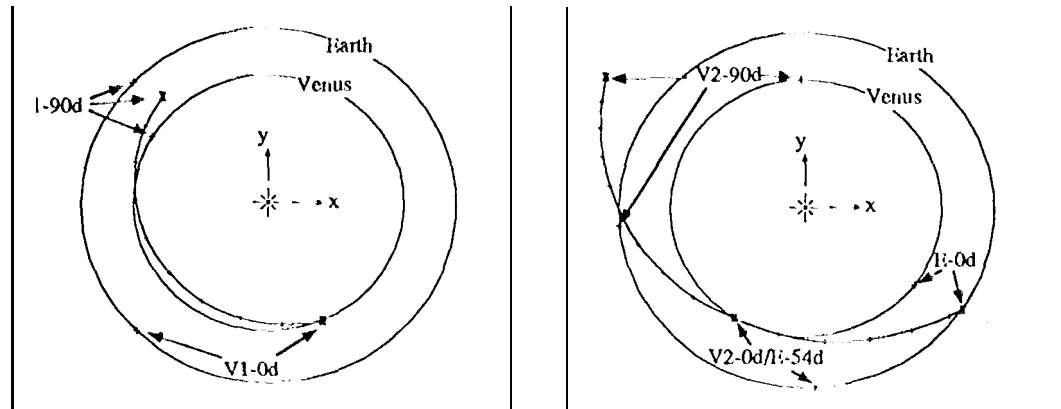


Figure 3 Ecliptic plane trajectory plots of the approach to Venus 1 (V1), Venus 2 (V2), and Earth (E) flybys. Vernal equinox is along x axis.

Table 1: Baseline a priori covariances

Name	Uncertainty, (1.σ)	Comments
Estimated Parameters		
Spacecraft epoch state	Position: 1000 km Velocity: 1 m/s	Per axis
Stochastic non-gravitational acceleration	$1 \times 10^{-12} \text{ km/s}^2$	Per axis, 1 day batches, 7 day time constant
Constant non-grav acceleration	$1 \times 10^{-12} \text{ km/s}^2$	Per axis
Solar radiation pressure coefficients	5.4% radial 1.00% transverse	Percentage of nominal acceleration at Venus of $57 \times 10^{-12} \text{ km/s}^2$
Maneuvers	2% of nominal ΔV. Minimum of 5 mm/s	Per axis. See Table 2 for "—" nominal ΔVs.
Venus & Earth ephemerides	Venus: 7 km (RSS) Earth: 10 km (RSS)	Fully correlated. Slightly conservative
Considered Parameters		
Constant non-grav acceleration	$1 \times 10^{-12} \text{ km/s}^2$	Per axis, diagonal.
Solar radiation pressure coefficients	5.4% radial 1.0% transverse	Percentage of nominal acceleration.
Station locations	19 cm spin radius 23 cm z-height 20 cm longitude	Fully correlated.
Troposphere	4.5 cm	Zenith range delay
Ionosphere	5.0 cm day 1.0 cm night	Range delays, X-band
Quasar position	$50 \times 10^{-9} \text{ Rad}$	R.A. & Dec

Table 2: Baseline maneuvers

Trajectory Correction Maneuver	Time	Nominal Δv (m/s)
2	V1-60d	1.8
3	V1-20d	0.13
6	V2-60d	0.13
7	V2-20d	0.11
8	V2+10d/ E-44d	68.
9	E-30d	6.3
10	E-10d	0.15

Table 3: Baseline data schedules and weights on approaches to flybys

Data Type	Tracking passes vs. F (lyby) times.		1 σ Noise	Comments
	F-90d to F-50d	F-50d to F-2d		
Baseline data types				
Cohorent Doppler	1/day	2/day	0.1 mm/s for V2 & E 1.0 mm/s for V1. (60s count)	Horizon to horizon passes. Alternate northern and southern hemisphere stations. 1 measurement/hour.
Range	1/day	2/day	15m	Same passes as Doppler. 9 measurements/pass.
Additional data types				
Precision Range (PR)	1/day	2/day	1 m	Same as Flange, Estimate daily range biases Of 5 m for each station.
Two-station Difference Doppler (DD)	1/wk	3/wk	0.1 mm/s (60s count)	Alternate north-south and east-west baselines. 1 measurement per 30 minutes.
Differenced wide band VLBI (ADOR)	2/wk	3/wk	50 cm	Alternate north-south and east-west baselines. Estimate quasar locations. 1 measurement/baseline.

The baseline conditions for both data arcs are given in Tables 1- 3. In Table 1, parameters are separated into *estimated* and *considered* categories, where the *considered* parameters simulate systematic errors in modeling which are not improved by the filter. The a priori uncertainties of the non-gravitational accelerations acting on the spacecraft (except for the maneuvers) are divided between these categories in order to roughly account for incomplete modeling arising from the use of uncoupled attitude control thrusters and poor characterization of the action of solar radiation on the spacecraft surfaces and of acceleration due to thermal radiation. Additionally, part of the estimated non-gravitational parameters are treated stochastically. The root-sum-of-squares of the non-gravitational parameter uncertainties amounts to $4.7 \times 10^{-12} \text{ km/s}^2$, which is about 8% of the nominal acceleration at Venus due to direct solar pressure alone. The uncertainty of this uncertainty is fairly large, so some of the experimentation described below varies these assumptions. The other considered parameter uncertainties approximately reflect current capabilities.

The nominal sizes of the Trajectory Correction Maneuvers (TCMs) from which a priori Δv uncertainties are calculated are given in Table 2. Maneuvers prior to Venus 1 and 2 flybys are fairly small because of the length of each approach and the ability to execute the TCMs well ahead of the flybys, but the short arc of about 54 days between Venus 2 and Earth, coupled with the trajectory dispersion at Venus 2, require large maneuvers with corresponding large effects on the OD as will be seen below. This puts additional importance on the OD delivery at Venus 2, since smaller dispersions will be reflected into both smaller Δv requirements and better OD knowledge post Venus.

Data types and quantities required by navigation are given in Table 3 (except that Precision Range is not currently required*). Only standard X-band Doppler and range data were used in the baseline case, but experiments were done using the additional data types to see if their use is justified,

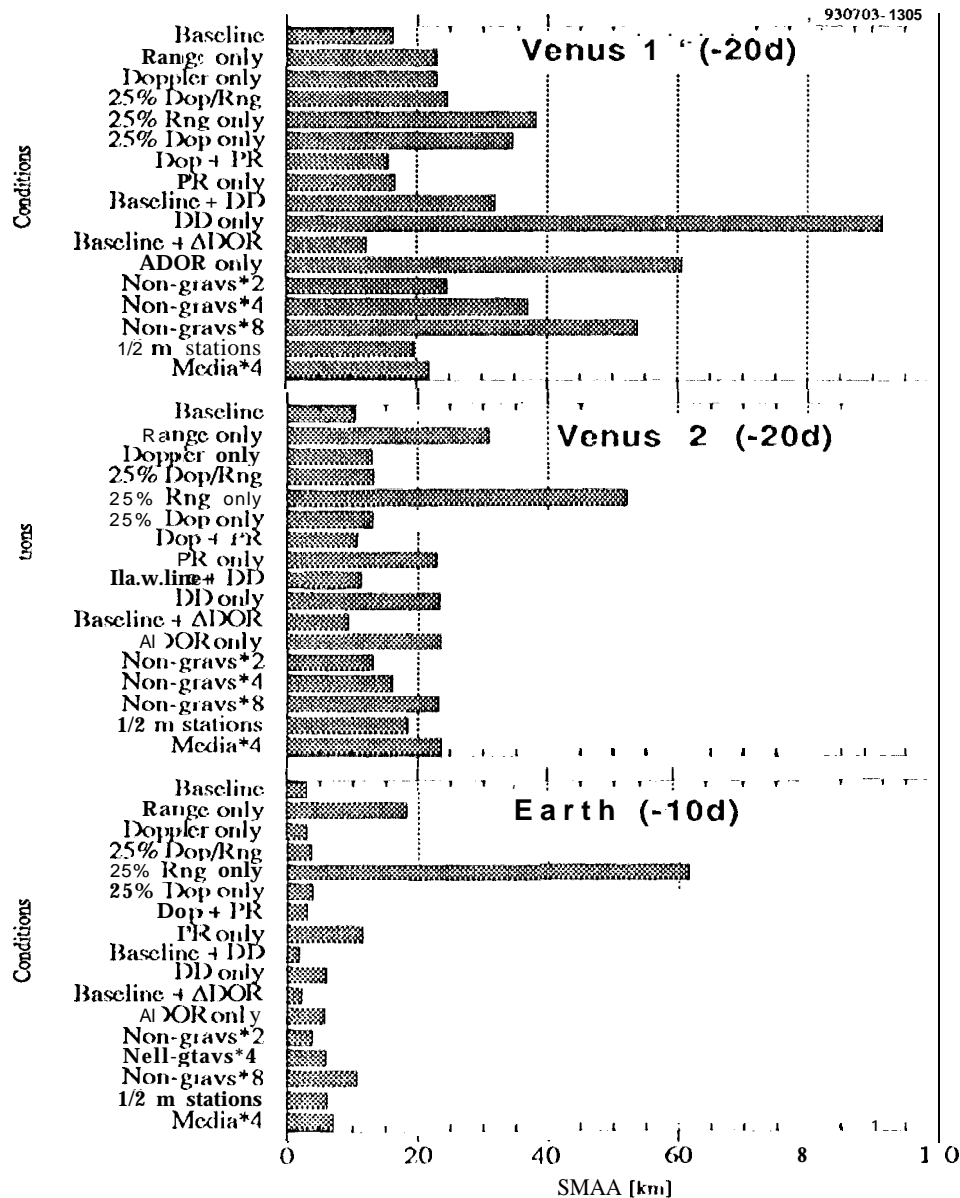


Figure 4 Comparison of size of the B-plane 10 error ellipse semi-major axis for each variation, each flyby.

* The "Differenced Range" data type is required but operationally expensive because it requires two station simultaneous ranging. Precision Range is nearly equivalent in function and performance, and needs only a single tracking station at a time. Thus, the requirement for Differenced Range will probably be replaced by a requirement for Precision Range.

Variations and Results

Figure 4 gives the list of experiments that were accomplished relative to the baseline setup and the results in terms of the size of the OD error at the last maneuver time before each flyby. The OD error is expressed as the size of the semi-major axis of the 10 error ellipse in the B-plane. (See Appendix). OD performance was found to be fairly robust for all reasonable variations, and the delivery uncertainties are well below the adopted 50 km reference and thus adequate for each flyby.

The poorest performance is found at Venus 1, due in part to the small absolute declination ($\delta < 10^\circ$) over most of the approach, as seen in Figure 5. The geometry is more benign for Venus 2 and Earth. The Doppler data loses much of its power to determine declination from the diurnal signature because of the well known approximate dependency of the uncertainty on $1/\sin(\delta)$.² Worse, platform modeling errors such as station locations, or errors which can masquerade as platform errors in the diurnal signature, such as media delays, can actually drive the solution away from the correct declination. Such was found to be the case for the approach to Venus 1 in an early phase of the analysis; data added beyond VI--30 days caused the uncertainty to dramatically increase through the action of the considered station location and media parameters on the Doppler signature. This was "cured" by deweighting the Doppler - assuming 1 mm/s noise (1σ) instead of the 0.1 mm/s used on the other two approaches. The preferable way to remedy this problem is to improve modeling, but this can cost money, and in this instance deweighting may be the, more practical -- although not optimum -- method.

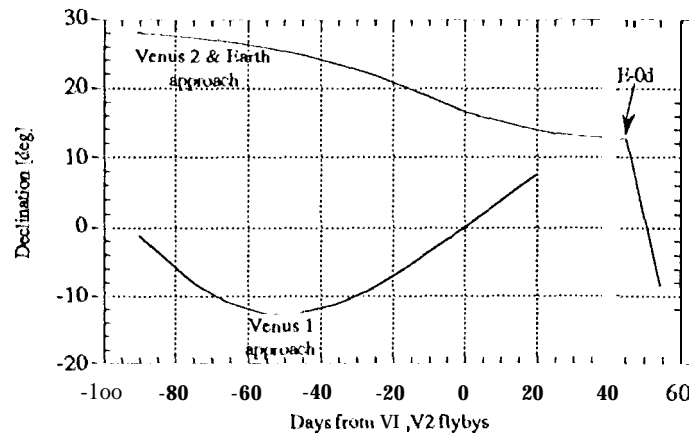


Figure 5 Spacecraft geocentric declination for the approaches to Venus 1, Venus 2, and Earth.

The "Range-only" variations on the baseline were done mainly to determine the capability of range data to independently generate good OD solutions as a cross-check against Doppler data. It is not unusual in operations to find that solutions using different subsets of data types disagree significantly; if one of the subsets can be identified as erroneous, then the others can be used. "Doppler-only" variations were run for the same reason. Figure 4 shows that range data alone provides an excellent cross-check against Doppler for the Venus 1 approach, but performs less well for the other approaches.

To determine the feasibility of reducing data quantity, the baseline solution was repeated using 75% of the number of scheduled range and Doppler tracking passes. Little difference was seen in the results for Venus 2 and Earth, but for Venus 1 the uncertainty increased from 16 km to 25 km. The Doppler-only and Range-only scenarios were also repeated at these reduced pass rates. Again, the results varied substantially between the data arcs, with the Range-only case performing abysmally for Venus 2 and Earth, but about the same as the Doppler-only case at Venus 1.

Experiments with enhanced data types were done by augmenting the baseline with them (except that Precision Range replaced normal range instead of augmenting it). These data types were also used independently to evaluate their capability to cross-check Doppler and Hinge.

The Precision Range (PR) data type consists of ordinary range data that is better calibrated and with which a different filter technique is used: a station-by-station, pass-by-pass range bias is estimated. Precision Range implicitly usgs long baseline.s (e.g., by interspersing tracking passes from northern and southern hemisphere stations and by tracking over long passes at a single station) to yield angular accuracy approaching that of VI .BI.³ Its performance does not deteriorate at zero declination. Figure 4 shows that baseline results with Precision Range changed negligibly, but that PR-only solutions performed somewhat better than Range-only solutions for all three flybys. In experiments not shown here, PR-only solutions using 25% of the passes in Table 3 generate considerably better results than the corresponding Range-only solutions (25 km vs. 52 km for Venus 2; 32 km vs. 62 km for Earth).

Differenced Doppler (DD) is obtained by differencing normal coherent Doppler measurements made simultaneously from two stations. Like Precision Range, its performance can also approach that of VI .BI, except that it is subject to the same zero declination problem as Doppler.⁴ This problem is demonstrated for the solutions at Venus 1. Performance was good for the Earth encounter. For Venus 2, the performance was comparable to that of Precision Range.

Delta-Differential One-way Range (ADOR) is a differenced spacecraft-quasar VI .BI measurement which yields extremely good angular accuracy, but brings considerable operational complexity and cost with it. ADOR performed comparably with DD and PR at Venus 2 and Earth, but better than for any other scenario at Venus 1 (except that ADOR-only performed poorly).

Sensitivities to errors in non-gravitational accelerations, station locations, and media calibrations were explored. All non-gravitational acceleration errors were increased by factors of 2, from a RSS total of 8% up to about 64% of the nominal acceleration due to direct solar pressure. The station location covariances⁵

about 20 cm uncertainty, highly correlated - were replaced by uncorrelated covariances of about 50 cm uncertainty. The baseline troposphere and ionosphere media effects were multiplied by a factor of 4. Of all these, the acceleration variations for Venus 1 generated the largest changes in result%

Scenarios were selected from the above experiments to demonstrate OD uncertainties as a function of time relative to each flyby. For Venus 1, the "Non-gravs*2" scenario was chosen as a slightly conservative example. For Venus 2 and Earth, the "25% Doppler/Range" scenario was selected. The results are shown in Figures 6-8. These illustrate the entirely different characteristics of each approach. Of particular interest in the Earth approach is the large effect of the maneuver errors at 11-44 and 11-30 days. Although the recovery times are quick and not greatly affected by the reduction in tracking data, it is obvious that the encounter will be operationally challenging. The B-plane error ellipses at the final maneuver times (before maneuver errors are applied) are shown in Figure 9, scaled up in order to be visible in the figure.

In summary, OD deliveries for the prime mission VVEJGA trajectory can be accomplished comfortably within the self-adoppti 50 km 1 σ criterion, and relaxation of requirements on tracking data can be supported. The requirement for Doppler/range tracking passes can be safely cut in half for Venus 2 and Earth, but probably should be kept at the current level for Venus 1 considering the sensitivity to non-gravitational accelerations and the short time after launch (7 months) in which to characterize these and other aspects of spacecraft performance. The Differenced Doppler and ADOR data types do not seem necessary, primarily because they add little capability compared to the operational cost and complexity added by simultaneous tracking from two stations (particularly for ADOR, which brings a host of other requirements into the problem as well). Use of Precision Range, however, is probably justifiable because of the improved cross-checking capability it brings to the reduced data scenarios versus relatively small operational costs and complications.

Variations of the prime mission trajectory due to different launches within the launch period should have small effect on the results given here. The secondary and backup missions have not yet been analyzed, but the broad results should be the same with the following major exception: there are a few flybys in which the declination problem is worse than for Venus 1. In those instances, Doppler could prove nearly useless in determining declination, and it may be desirable to maintain a requirement for ADOR as a compliment to range data.

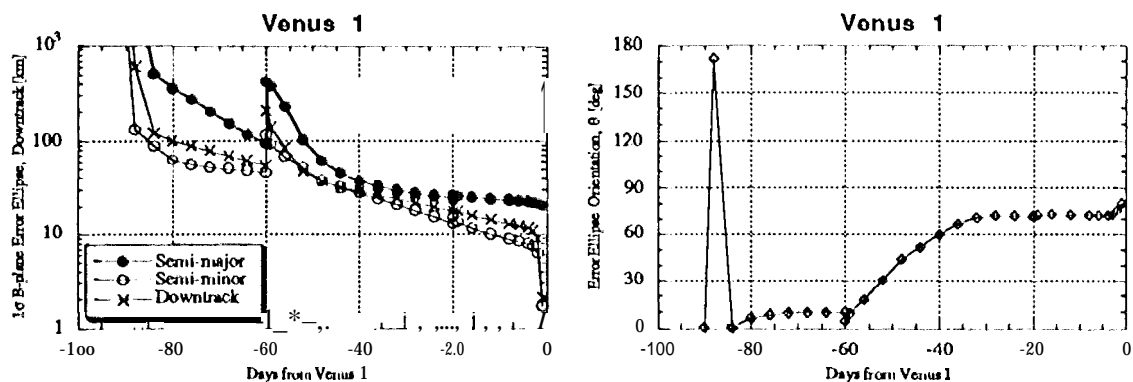


Figure 6 B-plane error ellipse (1 σ) and down track uncertainty as a function of time for the approach to the Venus 1 flyby. Ellipse semi-major and semi-minor axes are given. θ is a clockwise rotation of the major axis from the B-plane T axis (which is in the ecliptic plane).

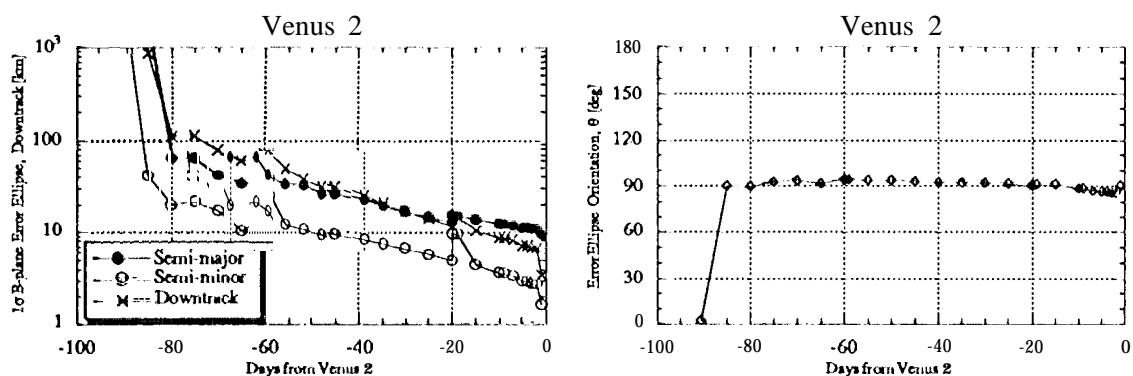


Figure 7 Error ellipse and down track uncertainty for approach to the Venus 2 flyby.

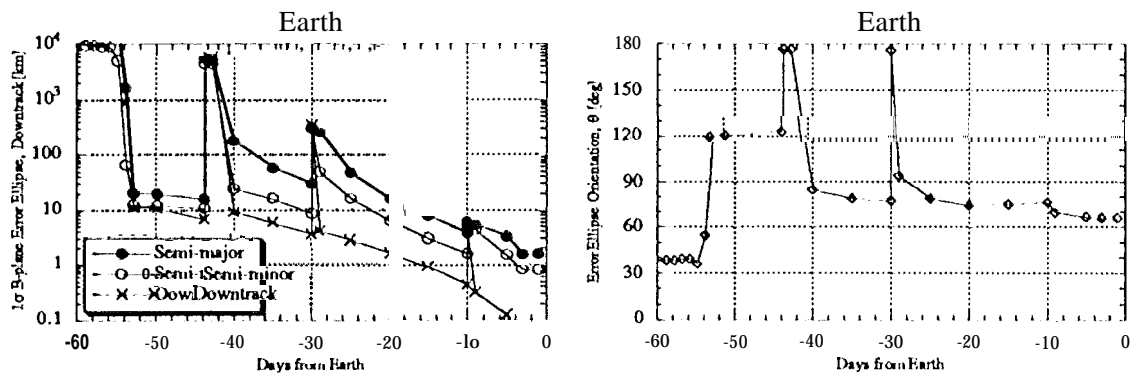


Figure 8 Error ellipse and down track uncertainty for approach to the Earth flyby.

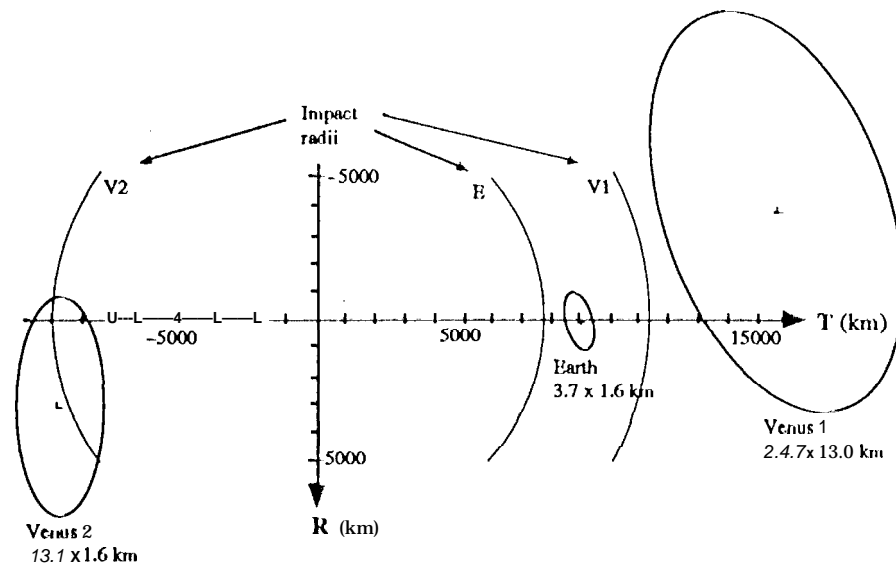


Figure 9 Error ellipses (1σ , scaled up by 300) in the B-plane coordinate system, along with the planet impact radii mapped into the same system. T axis is in the ecliptic plane. Ellipses are at final maneuver times (V1 -20d, V2-20d, & E-1 Od) for Venus and Earth flybys.

APPROACH TO SATURN

Following the trajectory for the prime mission, the Cassini spacecraft will approach the Saturn system in the first months of 2004. C10CSL approach to Saturn will occur on 25 June 2004 at which time the Saturn Orbit Insertion (SOI) maneuver will be performed to place the spacecraft in its initial orbit around the planet. For the purposes of OD analysis, the Saturn approach phase was assumed to cover the period beginning at SOI- 90d and continuing to SOI+ 7d. The spacecraft trajectory for this phase is shown in Figure 10. The plot on the left in the figure covers the entire approach period; the plot on the right shows only the two days around SOI but includes the orbits of the first 7 satellites, Mimas through Hyperion. Significant events during approach include a flyby of the satellite Phoebe at SOI- 19d, the final Saturn targeting maneuver at SOI- 17d, the SOI maneuver itself and a "cleanup" maneuver at SOI+5d.

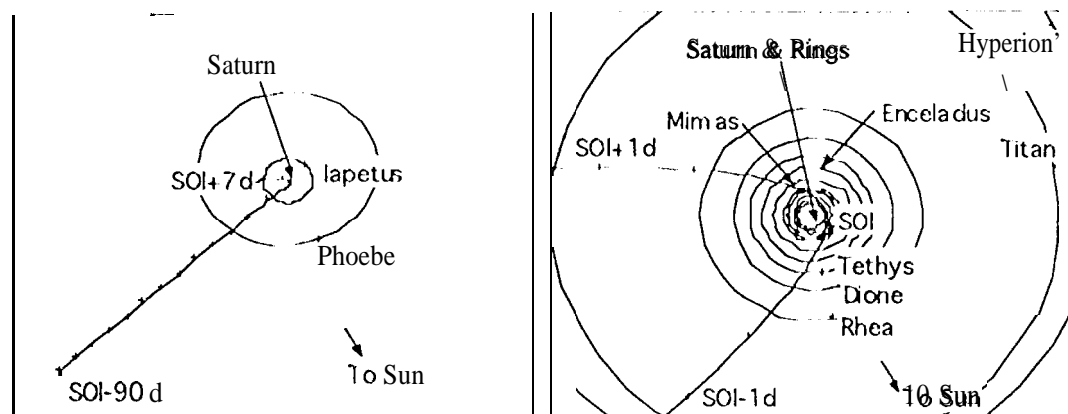


Figure 10 Cassini Saturn approach trajectory as seen looking down from Saturn's north pole.

Optical navigation data will be introduced in the mission's OD analysis during the Saturn approach phase. The optical data will consist of measurements of the positions of the Saturn satellites against known star backgrounds in images taken by the spacecraft's camera(s). These data will be combined with standard radiometric navigation data to improve the estimate of spacecraft target-relative position. The satellite ephemerides will also be updated as part of the OD estimation process.

The primary objective of the OD analysis for the approach phase was to characterize the basic capability as represented by spacecraft trajectory knowledge uncertainty just before the SOI-17d and SOI maneuvers. Uncertainties in satellite positions were also examined. OD performance for cases using only radiometric or optical data was investigated to compare the contributions of the different data types. The radio-only case was also of interest as a failure scenario assuming the spacecraft's cameras were inoperable. For this scenario, the use of enhanced radiometric data types was considered. The effects of reductions in the amount of optical and radiometric data were also addressed as were sensitivities to variations in the treatment of the optical data.

Table 4: Baseline a priori covariances for Saturn approach

Name	Uncertainty (10)	Comments
Estimated parameters:		
Spacecraft epoch state & Saturn (planet) ephemeris	Heliocentric spacecraft position: 400 km per axis, velocity: 0.1 m/s per axis Saturn epoch position: RSS 239 km	Correlations of spacecraft state parameters with Saturn epoch state parameters included for analysis in Saturn barycentered coordinates. Saturn ephemeris covariance at level expected for ground-based solutions in 2004.
Stochastic non-gravitational acceleration	$0.69 \times 10^{-12} \text{ km/s}^2$	Per axis; 6 hr batches, 1 day time constant.
Constant non-grav acceleration	$0.69 \times 10^{-12} \text{ km/s}^2$	Per axis, diagonal.
Solar radiation pressure coefficients	5.4% radial 1.0% transverse	Percentage of nominal acceleration. Nominal = $0.23 \times 10^{-12} \text{ km/s}^2$ at Saturn
SOI-17d & SOI-5d Maneuvers	1.7% of nominal AV	Per axis. Nominal AVS: 0.75 m/s for SOI-17d, 50 m/s for SOI-5d
SOI Maneuver	1% of nominal AV	Per axis. Nominal AV: 610 m/s.
Satellite ephemerides and masses, Saturn system mass and Saturn J2 gravity harmonic	RSS position sigmas for each satellite - Dione: 1387. km Rhea: 1430. km Titan: 1151. km Hyperion: 1450. km Iapetus: 2168. km Phoebe: 9402. km	Correlated where appropriate for satellite dynamic motion model (integrated Cartesian orbits and variational partials). Covariance at level expected for ground-based solutions in 2004. Software currently limited to 6 satellites.
Considered parameters		
Constant non-grav acceleration	$0.69 \times 10^{-12} \text{ km/s}^2$	Per axis, diagonal.
Solar radiation pressure coefficients	5.4% radial 1.0% transverse	Percentage of nominal acceleration.
Station locations	0.5 m spin radius, z-height, longitude	Diagonal, conservative.
Troposphere	4.5 cm	Zenith range delay
Ionosphere	5.0 cm day 1.0 cm night	Range delays. X-band
Quasar position	$50 \times 10^{-9} \text{ Rad}$	R.A. & Dec (for ADOF)
Satellite image centerfinding error	0.75% Titan; 0.20% icy satellites	Proportional to satellite image diameter; effective error 40 km for Titan

Table 5: Baseline data schedules and sigmas for Saturn approach

Data Type	Data Frequency		Sigma	Comments
	SOI 90d to SOI 30d	SOI 30d to SOI 7d		
Baseline Radiometric data				
Coherent Doppler	1 pass/day	pass/day	0.1 mm/s (60 s count)	Horizon horizon passes. Alternate northern and southern hemisphere stations.
Range	1 pass/day	1 pass/day	100 m	Same comments as Doppler.
Segmented Radiometric data				
Two-station Difference Doppler (DD)	1 pass/wk	pass per 2 days	0.1 mm/s (60 s count)	Alternate north-south and east-west baselines. 11 measurement per 30 minutes.
Difference wide-band VLBI (DDOR)	3/wk	1 per 2 days	50 cm	Alternate north-south and east-west baselines. Consider quasar locations.
Baseline Optical data				
Narrow angle (NAC) or wide angle (WAC) camera images	6/day	8/day	0.5 pixel	1/3 targetted for Titan; remainder targetted for one of 8 icy satellites: (NAC 6 prad/pixel: WAC 60 μ rad/pixel)
Titan images	15 WAC 120 NAC	88 NAC		
Icy satellite images	45 WAC 141 NAC	11? NAC		Dione, Rhea, Hyperion, Iapetus, Phoebe

Setup

The baseline conditions for the Saturn approach OD estimation are summarized in Table 4. In this case, the spacecraft epoch state and Saturn epoch state parameters are initially correlated since the estimation is performed in a coordinate system with origin at the Saturn system barycenter. The assumptions for treatment of non-gravitational accelerations and solar pressure parameters are similar to those used for the Venus and Earth flyby analysis. The three maneuvers are also handled in a manner similar that used in the previous analysis except that the values for the associated a priori uncertainties are somewhat different. The sizes and percentage uncertainties shown in the table represent the best estimates available at this time. It should be noted that the uncertainty for the SOI maneuver is by far the largest due to the size of the velocity change required to guarantee capture into Saturn orbit.

Parameters modeling the motion of the satellites are included in order to process the optical data. The planet and satellites are treated as a multi-body dynamic system generating dependencies among the satellite epoch states, Saturn system mass, satellite masses and the Saturn J2 gravity harmonic parameters. Additional consider parameters are also included to simulate systematic errors in processing these data. The image processing algorithms attempt to extract the center of the satellite image from the lit disk or crescent visible in the picture. This process is considerably more difficult for a body with an atmosphere such as Titan than for the other icy satellites lacking an atmosphere. For this reason, the centerfinding error consider parameters for Titan images have a larger a priori uncertainty than those for the icy satellite images.

The data types and assumptions on the quantity and quality of each type used in the approach OD analysis are summarized in Table 5. Radio tracking passes are scheduled each day during this period; optical navigation pictures are also scheduled on most days. Due to a limitation in the OD software,* images of only six satellites could be included in the optical data arc. The six outermost satellites -- Dione, Rhea, Hyperion, Titan, Iapetus and Phoebe -- have been chosen; this set includes satellites both inside and

* This limitation will be removed in the operational version of the OD software.

outside of Titan's orbit and the satellites with largest masses. Although Table 5 specifies the quantity of optical navigation data as number of images per day, there are some periods where no optical navigation images are scheduled to give priority to other spacecraft activities. These include gaps of ≈ 1 day for the SOI-17d and SOI-5d maneuvers, a gap of ≈ 2 days around the SOI maneuver and a gap of ≈ 1 day around Phoebe closest approach at SOI-19d.

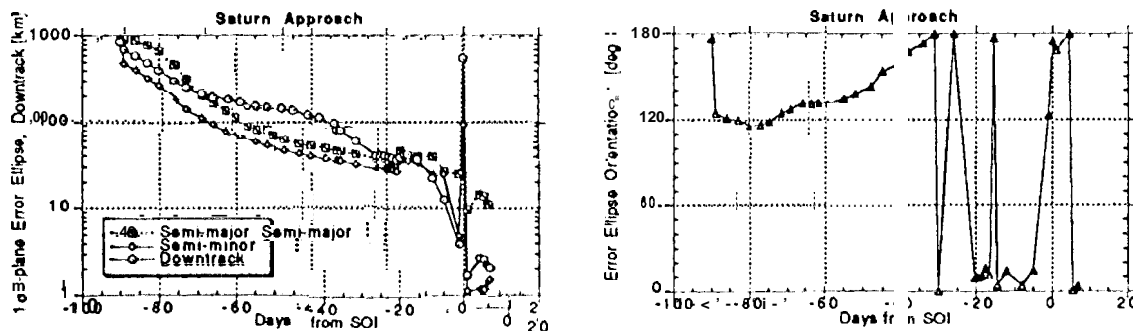


Figure 11 B-plane error ellipse parameters and down track uncertainty (1σ) as a function of time for Saturn approach.

Variations and Results

OD performance for the baseline case using Doppler, range and optical data is shown in Figure 11. Results are presented in terms of spacecraft state uncertainties mapped to the Saturn 13-plane at SOI. The spike in these curves at SOI is a transient effect due to the incorporation of the large SOI maneuver uncertainty. The behavior of these curves before SOI is the primary focus of the OD analysis. Of particular interest are the predicted OD errors at the data cutoff times of SOI-18d and SOI-5d. These cutoff times represent the latest opportunities for updating the OD solutions before the last Saturn targeting maneuver and the SOI maneuver itself. Figure 12 shows the 1σ B-plane error ellipses at these two times; the error ellipse at SOI-30d is also shown for comparison. As for the Venus and Earth flybys, there is currently no explicit requirement on the size of the OD uncertainty during the approach phase. The predicted baseline capability of 35.7 km for the B-plane semi-major axis at SOI-18d and 27.4 km at SOI-5d should be more than adequate to meet the current mission objectives for this phase.

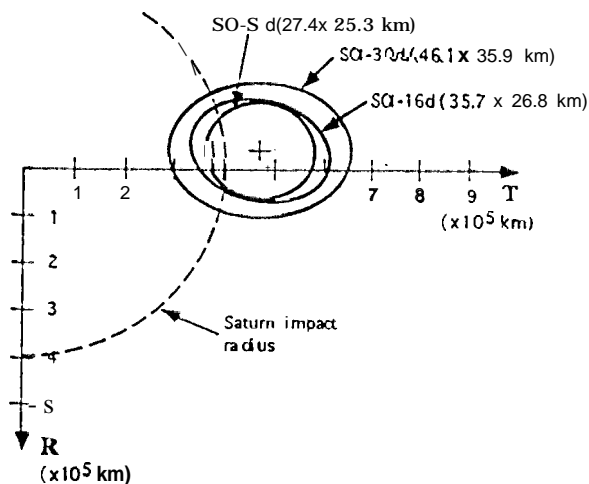


Figure 12 Error ellipses (1σ , scaled up by 4000) in the B-plane coordinate system for Cassini Saturn approach. (T axis in Saturn equatorial plane of date.)

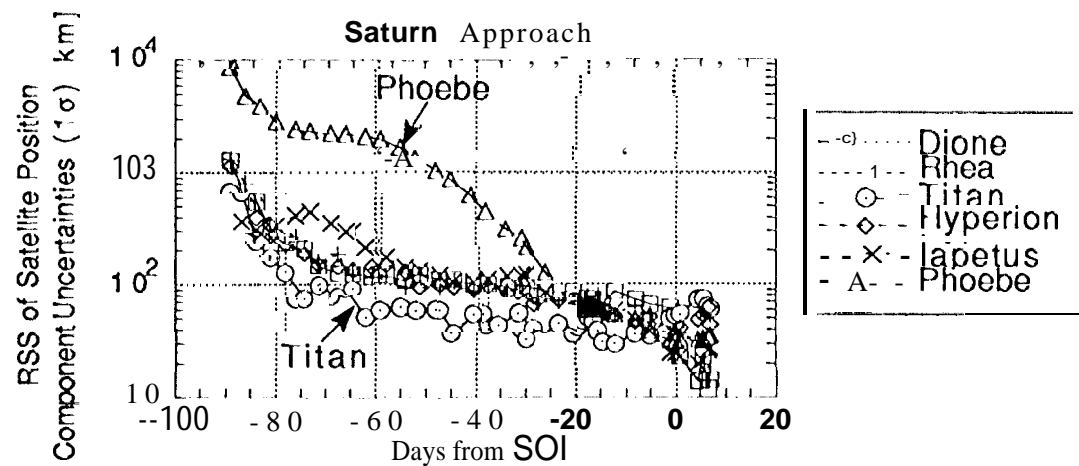


Figure 13 Satellite ephemeris convergence as a function of time for Saturn approach. FISS of position component uncertainties mapped to current time are plotted.

The Saturn approach optical data will provide the first opportunity to update the satellite ephemerides from the ground-based orbit solutions. Figure 13 shows the predicted improvement in position uncertainties for the six satellites included in the baseline OD estimate. The RSS value of each satellite's position component uncertainties at data cutoff times throughout the approach phase arc plotted. All satellites show a continuous decrease in position uncertainty as more optical data is incorporated. Within a few days of SOI, all satellite position uncertainties have been reduced to 4080 km. Titan has the smallest uncertainty prior to SOI due to its smaller a priori uncertainty and to the larger number of optical data points used in the estimation. A large reduction in Phoebe's uncertainty occurs after the flyby on SOI-19d.

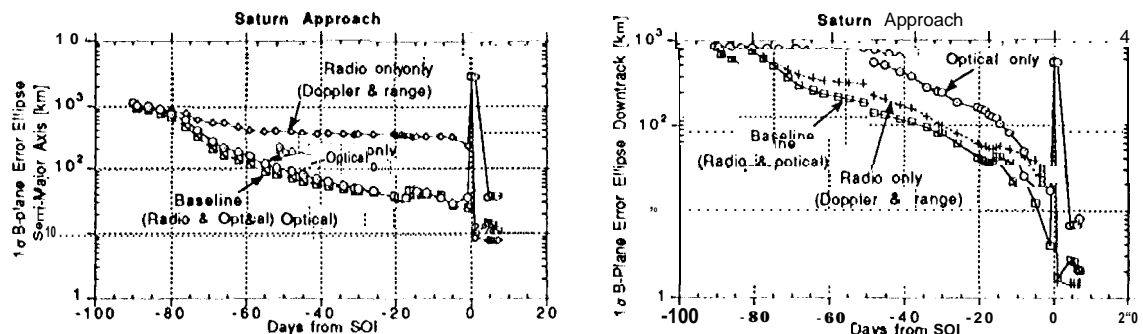


Figure 14 B-plane semi-major axis and down track uncertainty (1σ) as a function of time for cases using only radiometric or optical data for Saturn approach.

Figure 14 gives a comparison of OD performance using only radiometric or optical data against the baseline case. The curves in this figure clearly illustrate the contributions of each data type to the overall OD capability. Optical data is required to reduce the B-plane semi-major axis to a few tens of kilometers by SOI-5d. The radiometric data can only reduce this to a few hundred kilometers in the same time period. Conversely, radiometric data is required to reduce the downtrack uncertainty which is related to the time of Saturn closest approach. The downtrack uncertainty remains above 100 km until SOI-10d using only optical data whereas values under 100 km are achieved after SOI-30d using radiometric data. The baseline case reflects the benefits of both data types, performing as well or better than the other two cases throughout the entire data arc.

Figure 15 gives the results of other variations from the baseline case investigated for this study. Values of the semi-major axis of the 1σ Saturn 11-plane error ellipse at SOI-18d and SOI-5d are plotted.

The variations can be grouped into four sets as indicated in the figure. The first two sets address OD performance using only radiometric data. These cases explore sensitivity to the station location and atmospheric media consider parameters and potential improvements from the addition of two enhanced data types - Differenced Doppler and DDOR. The results of these simulations indicate that the a priori station location uncertainty is the most important factor influencing OD performance in the radio-only scenario. A reduction by a factor of 2 in the R-plane semi-major axis can be achieved by excluding these parameters or by using a more realistic a priori uncertainty which includes correlations between station locations at the different sites. In contrast, relatively little improvement is obtained by adding Differenced Doppler or DDOR to the baseline Doppler and range data regardless of the treatment of the consider parameters. The current requirements for these data types during the approach phase can probably be eliminated. Although not evident in Figure 15, standard range data also plays a major role in approach OD performance by reducing the downtrack uncertainty. At SOI-18d, the case using only Doppler data has a downtrack uncertainty of 227 km; this is reduced to 54 km when range data is added.

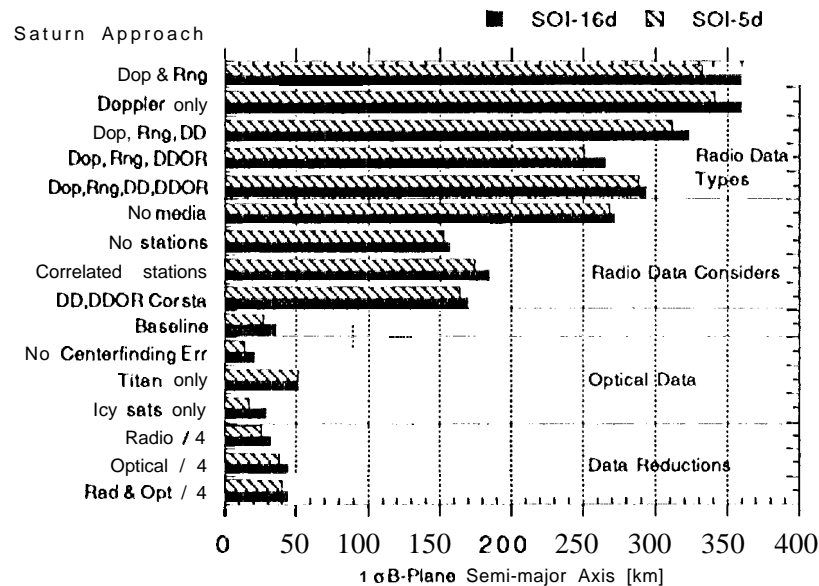


Figure 15 Comparison of 1σ B-plane error ellipse semi-major axis for variations in approach OD analysis.

The third set of variations for this analysis is concerned with the optical data. Sensitivity to the centerfinding error consider parameters is addressed along with the relative influence of the Titan images as compared to the images of the icy satellites. The values shown in Figure 15 confirm that the Titan centerfinding error consider parameters make a significant contribution to the overall OD error. A 10 km reduction in B-plane semi-major axis is achieved when the centerfinding error consider parameters are excluded from the estimation. An improvement in performance compared to the baseline case is also seen when only the icy satellite images are used. Conversely, B-plane errors increase from the baseline values when only Titan images are included. These results highlight the importance of the on-going effort to improve the Titan atmosphere model used in processing the optical navigation pictures. The Titan data can be of greater benefit if centerfinding errors can be reduced below the levels assumed in this analysis. Future studies should also investigate better characterization of these centerfinding errors in the OD filtering process. If problems with the Titan optical data cannot be eliminated, it appears feasible to use only icy satellite images for all or parts of the approach data arc.

The final set of variations to be presented involve reductions in the amount of data used in the OD estimation. Simulations were done using data arcs that reduced the amount of radiometric and/or optical data by a factor of 4 from that used in the baseline case. The values in Figure 15 show that there is very little change in OD performance when the amount of Doppler and range data is decreased. Some reduction

in the requirements for radiometric tracking passes during approach seems feasible given the results of these cases. A performance degradation is observed, however, for the cases where the number of optical navigation images is decreased, 11-plane semi-major axis values increase by 41 % at SOI- 30d, 25% at SOI- 18d and 48% at SOI-5d when fewer images are included in the estimation. The impact of this degradation is unclear at this time since there are no true requirements on the approach OD accuracy. It may be acceptable if a significant reduction in operational costs would result by taking fewer optical navigation pictures.

HUYGENS PROBE DELIVERY

After the SOI maneuver in June 2004, the combined Cassini-Huygens spacecraft enters an extended orbit whose major axis is about 90° off the sun line as shown in Figure 16. A periapsis raise maneuver is accomplished near Saturn apoapsis, and the combined spacecraft begins the approach to Titan. About 21 days before Titan, the Huygens Probe and the Orbiter separate from each other, leaving the Probe on an impact trajectory. Two days later the Orbiter performs a large deflection maneuver in order to move off the impact trajectory and increase spacing so that it arrives several hours after the Probe. The Probe enters Titan's atmosphere 155 days after SOI, in November 2004, and the Orbiter follows, receiving and recording telemetry as the Probe descends through the atmosphere and impacts the surface. The Orbiter continues by Titan, making a closest approach of 1 500 km altitude.

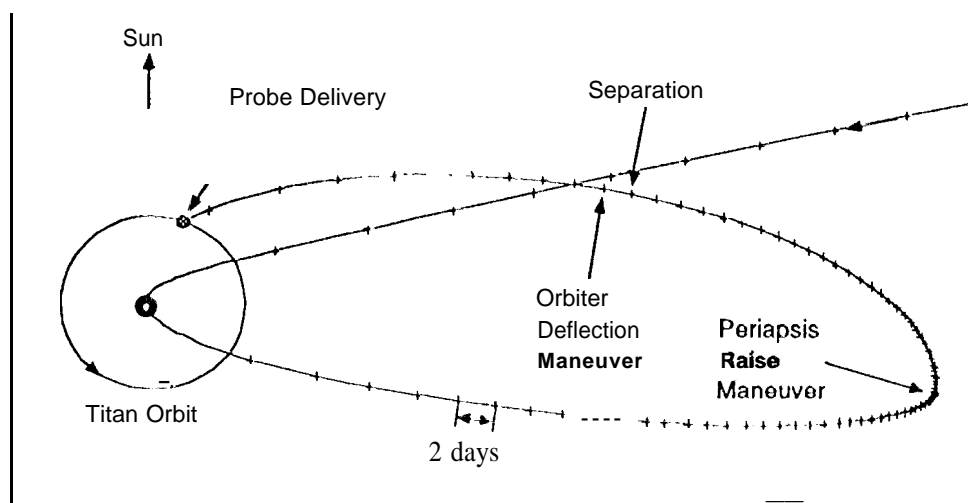


Figure 16 Nominal First Orbit and Trajectory for Huygens Probe Delivery.
Trajectory plane view.

The nominal first orbit is shown in Figure 16. The analysis was based on an earlier scenario in which the orbit was similar but rotated counterclockwise about 25° closer to the sun-line. The trajectory differences should have little impact on the major results. Tables 6 through 8 give the conditions used for a data arc which begins about 10 days before Saturn apoapsis. Although Differenced Doppler and ADOR data types were included in baseline solutions, the Doppler and optical data types were the work horses for OD, with Doppler tying the spacecraft to the system barycenter through the gravity signature, and the Optical data tying the spacecraft to Titan. Removing Differenced Doppler and ADOR had an indistinguishable effect on the results. Removal of the range data also had negligible effect. A limitation of this analysis is that only Titan optical data was simulated; none was used for the other satellites. Inclusion of the other satellites may improve Titan-relative OD somewhat, since correlations between their ephemerides and Titan's should act to improve Titan- relative navigation.

Table 6: A priori covarlances

Name	Uncertainty (1 σ)	Comments
<i>Estimated parameters</i>		
Epoch state	Position: 150 km Velocity: 60 mm/s	Per axis
Maneuvers	See Table 7	Per axis.
Saturn ephemeris	Position: 1190 km Velocity: 14 mm/s	RSS (Correlated covariance). Conservative
System mass (GM)	100 km ³ /s ²	
Saturn J2	.001	
Titan ephemeris	Position: 900 km Velocity: 4 m/s	Per axis.
Titan mass	10 km ³ /s ²	
Stochastic non-gravitational acceleration	2 x 10 ⁻¹² km/s ²	Por axis. 2 day batches, 2 day time constant.
<i>Considered parameters</i>		
Optical center-finding error, Titan.	60 km	Per axis (pixel & line).
Constant non-gravitational acceleration	1 x 10 ⁻¹² km/s ²	Per axis
Solar radiation pressure coefficients	8.5% radial 3.4% transverse	Percentage of nominal acceleration. Nominal = 0.2 x 10 ⁻¹² km/s ²
Station locations	45 cm spin radius 45 cm z-height 46 cm longitude	Uncorrelated
Quasar position	50 x 10 ⁻⁹ Rad	For ADOR. R.A. & Dec
Troposphere	6 cm	Zenith range delay

Table 7: Maneuver errors (1 σ)

Maneuver	Time (days)	Ave error (mm/s)
PRM (Periapsis Raise Maneuver)	T-68	7000
PRM Cleanup	1-53	120
PDM (Probe Delivery Maneuver)	T-23	20
Probe separation	1-22	10
Deflection Maneuver	1-20	750
Deflection Maneuver Cleanup	T-15	15
Orbiter Delivery Maneuver	T-5	20

Table 8: Data schedules and weights

Data Type	Schedule	Weight (1 σ)	Comments
Coherent Doppler	Average 1 pass/day until T-36d; then continuous.	0.5 mm/s (60s count)	Horizon to horizon passes. 2 hour count.
Range	Same as Doppler.	100m	Same passes as Doppler. 1 point per pass.
Optical	4/day until T-7d; then none.	6 x 10 ⁻⁶ Rad (1 pixel)	Narrow Angle Camera
Difference Doppler	1 per 2 days	0.2 mm/s (60s count)	3 hour count.
ADOR	1 por 2 days	15 cm	Alternate north-south and east-west baselines.

One of the objectives of the OD analysis was to determine the Titan relative uncertainty as a function of time. This information is used in the mission design process of choosing the Probe separation time. There are two competing desires in choosing the separation time: 1) release the Probe as late as possible so that the delivery uncertainty is smallest, and 2) release the Probe as early as possible so that the Orbiter can safely maneuver away from the impact trajectory. Figures 17 and 18 show the size of the Titan centered target plane error ellipse and downtrack uncertainty as a function of time. Figure 17 shows results for the Probe-Orbiter combination when no maneuvers are executed after the Periapsis Raise Maneuver cleanup at T(titan) -53 days. For a given data cut-off, the OD knowledge is frozen, a Probe Delivery Maneuver is designed and executed based on this knowledge, after which the Probe Separation Maneuver occurs. The total delivery error to Titan for the Probe, then, is the OD uncertainty at the data cut-off time combined (RSSed) with maneuver execution errors amounting to about 40 km. For a data cut-off at T-25 days, this yields a 1 σ error ellipse with a semi-major axis of 156 km aligned along T, and a semi-minor axis of 48 km.

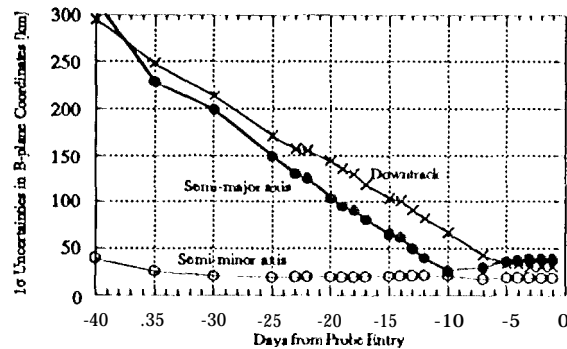


Figure 17 Titan centered B-plane for Probe-Orbiter combination as a function of time.

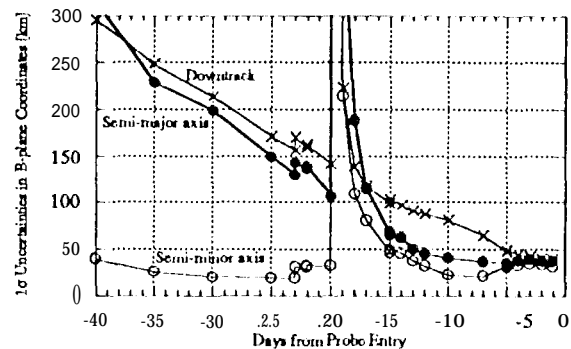


Figure 18 Titan centered B-plane for Orbiter with maneuvers at 23, 22, 20, and 5 days before Probe entry.

Figure 18 shows the Orbiter uncertainties for the choice of T-25d data cut-off. Based on a data cut-off at T-25 days, the Orbiter and Probe separate at T-22 days after which time the Probe delivery error is fixed at the values given above. The Orbiter executes the Deflection maneuver at T-20 days, resulting in a 1 σ error of about 1800 km. Within 5 days the OD knowledge recovers with tracking data to approximately the level prior to the maneuver. A cleanup maneuver removes the errors induced by the Deflection maneuver and tweaks the final Orbiter delivery. The Orbiter 10 error ellipse for a data cut-off at T-5 days (which is at or near the last delivery time) has semi-axes of 35 and 31 km.

A representative 11-plane geometry for the Probe and Orbiter deliveries is shown in Figure 19. The Probe is currently targeted to a point 80° counter-clockwise from the T axis at a radius from the origin which corresponds to an entry angle of 64°. * Also mapped into the B-plane are the desired lower and upper limits for the Probe entry angle. The nominal target in the figure was chosen in an early scenario in order to accommodate a skinny error ellipse (not shown) between the entry angle limits. Because the long axis was along T, this dictated a high latitude. The current probe delivery error ellipse is somewhat smaller than the one used to locate the nominal target, but with similar orientation. Because of the reduced size, it is now possible to target to lower latitudes if the project should desire to do so. To explore this possibility, a Monte Carlo Gaussian distribution of 2000 points was generated to obey the statistics of the Probe's 156x48 km delivery error ellipse based on a data cut-off at T-25 days. The zero point of this distribution was moved in the B-plane as far clockwise as possible until the dispersion exceeded the entry angle limits by an arbitrarily chosen 1% on each side. The exercise demonstrated that for this level of risk the Probe can be targeted to 60° counter-clockwise from T, at an

* The "entry angle" is the angle between the trajectory and a tangent plane to the sphere at the penetration point. The Cassini Navigation team delivers the Probe to an interface altitude chosen to be well above the atmosphere, after which the Huygens team assumes responsibility for the descent to impact.

entry angle of **63.3°**. The target point could be brought further clockwise if the size of the error ellipse were **decreased** or if the probability of success were **reduced**. The size of the error ellipse can be decreased either by delaying the Probe separation time, or by reducing the slope of the curves (mainly the semi-major axis) in Figure 17. This will be discussed in a following paragraph. Figure 19 also shows the Orbiter dispersion based on a data cut-off at T-5 days. The aim point for the Orbiter is only **representative** since the placement can vary with different mission scenarios (except in the radial direction, which is fixed by the planned flyby altitude of 1500 km).

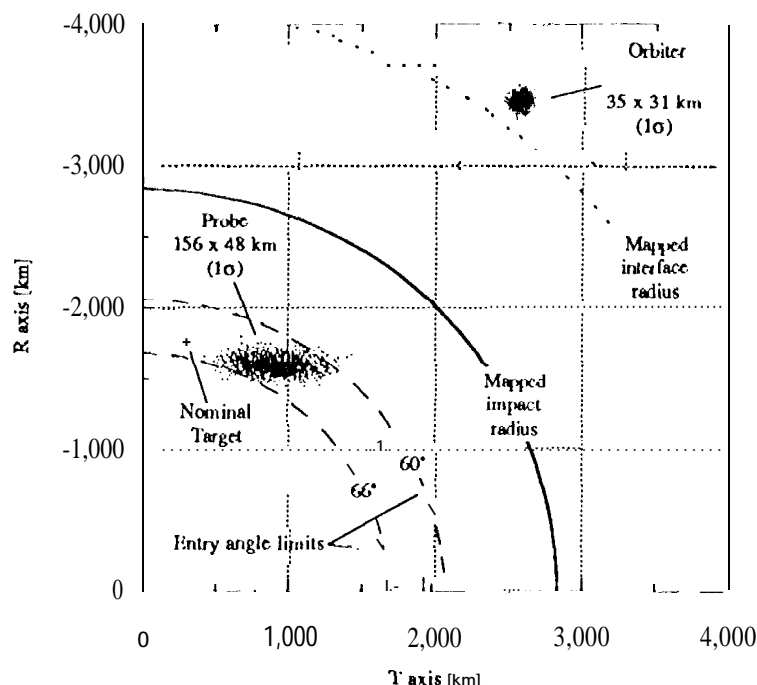


Figure 19 Probe and Orbiter Monte Carlo dispersions in the Titan B-plane.

Sensitivities were explored for variations in data weights, data schedules, and the a priori covariances of Table 6. The largest effect by far for reasonable variations was found to be due to the Titan center-finding error. When solutions were run using 30 and 95 km center-finding error instead of the nominal 60 km, it was found that the nearly straight-line behavior of the curve for the semi-major axis (Figure 17) between T-1 O and T-30 days was retained, but the slope and intercept values in a straight-line approximation, $SMAA = a + b t$, changed nearly proportionally with the size of the error. An approximation which gives 10-20% answers for center-finding errors between 30 and 95 km is given by

$$SMAA = CFE(-1.1 - 0.1S t)$$

where CFE is center-finding error in km, t is in days from Probe entry, and SMAA is in kilometers. This is completely invalid after 3--10 days where the uncertainties level off.

Experiments were also done using only optical or radio data. For the radio-only case, the Titan-relative OD was no better than the a priori satellite ephemeris uncertainty, since the radiometric data primarily ties the spacecraft to the system barycenter through the gravity signature. The Orbiter-Probe combination did not come sufficiently close to Titan on the first orbit to significantly improve the ephemeris uncertainty through the satellite's gravity signature. However, as indicated by analysis in the tour phase, it should be possible to tie the spacecraft to Titan through the gravity signature of the first encounter (with a somewhat increased flyby altitude for safety), delivering the Probe on a subsequent encounter. The optical-only solutions exhibited large uncertainties in the Titan B-plane until late in the encounter. The semi-major axis of the error ellipse was 491 km at T-25d, not going below 150 km until after T-17d. This scenario, although better than the radio-only case, is not attractive for Probe delivery on the first orbit.

The next phase of analysis for the **Huygens** probe delivery will use the latest trajectory to verify the results discussed above. Additionally, optical data for most if not all of the major satellites will be used. The satellite ephemeris model will also be changed, using integrated Cartesian orbits and variational partials instead of the conic modeling used thus far.

CONCLUSIONS

Orbit Determination for the inner solar system phase was found to be robust, with 1 σ knowledge uncertainties of 25 km or less for Venus and Earth flybys under most reasonable assumptions. The number of passes for standard Doppler and range data types can be safely reduced by half during the intense data periods beginning 90 days before each flyby, with the exception of the Venus 1 approach where there was found to be some sensitivity to pass frequency. There is little need for two-station simultaneous data types such as Differenced Doppler and ADOR, except that ADOR data might prove useful for low declination flybys on contingency missions. The Precision Range data type can probably be justified on the basis of somewhat improved OD performance versus low implementation and operations costs. Future analysis will focus on the period from launch to the first Venus flyby in the prime mission, and on low declination geometries for flybys on the contingency missions.

On the approach to Saturn, standard Doppler, range, and optical data make possible a 1 σ delivery of about 35 km to the Saturn target plane based on a data cut-off 18 days before the encounter. Standard radiometric and optical data were demonstrated to complement each other, with optical data determining target plane position, and radiometric data determining arrival time. Little need was found for enhanced data types such as Differenced Doppler, ADOR, and Precision Range. Some reduction in the quantity of radiometric data seems feasible, but there can be a significant loss of performance if optical data is reduced.

A typical 1 σ Probe delivery to the Titan target plane is 156 km, based on a data cut-off 25 days before Titan. The Orbiter delivery, for data until 5 days before Titan, is about 35 km. A large sensitivity to Titan optical center-finding error was demonstrated. No need for enhanced data types, such as Differenced Doppler, ADOR, or Precision Range, was found. Future analysis should concentrate on Probe-Orbiter relative Orbit Determination in support of the telecommunications link between the two spacecraft during Probe descent through Titan's atmosphere. Additionally, enhancements to the simulation should be made, such as using more satellites in addition to Titan for optical data, and using more realistic satellite ephemerides and variational partials.

References 6 and 7 are included in the Reference section for completeness, since they are the original source of much of the material presented here.

ACKNOWLEDGEMENTS

The authors thank Jeremy B. Jones of JPL for fruitful discussions on goals and motivations for this analysis, and Francis M. Stienon, also of JPL, for maintaining and troubleshooting the ATHENA software set used for much of the analysis.

The research described in this paper was performed at the Jet Propulsion Laboratory, California Institute of Technology, under contract with the National Aeronautics and Space Administration.

REFERENCES

1. "Cassini Project Mission Plan", Project Document 699- 100-2 Rev B (internal document), Jet Propulsion Laboratory, Pasadena, California, 12 March 1993.
2. Hamilton, T.W., and Melbourne, W.G., "Information Content of a Single Pass of Doppler Data from a Distant Spacecraft", JPL Space programs Summary 37-39, Vol. III, March-April 1966, pp. 18-23.

3. Thurman, S.W., McElrath, T.P., and Pollmeier, V. M., "Short-arc Orbit Determination Using Coherent X-band Ranging Data", Paper AAS 92-109, AAS/AIAA Spaceflight Mechanics Meeting, Colorado Springs, Colorado, 24-26 February 1992.
4. Thurman, S.W., "Deep-space Navigation Performance of X-band (8.4 GHz) Differenced Doppler Data", JPL Engineering Memorandum 314-486 (internal document), Jet Propulsion Laboratory, Pasadena, California, 24 July 1990.
5. Folkner, W.M., "DE234 Station Locations and Covariance for Mars Observer", JPL Interoffice Memorandum 335.1-92-013 (internal document), Jet Propulsion Laboratory, Pasadena, California, 76 May 1992.
6. Taylor, T., "Cassini/Huygens Probe and Orbiter Error Analysis", JPL Interoffice Memorandum 314.3-978 (internal document), Jet Propulsion Laboratory, Pasadena, California, 14 June 1991.
7. Taylor, T., "OD Results for Cassini Inner Solar System Flybys", JPL Interoffice Memorandum 314.3-1066 (internal document), Jet Propulsion Laboratory, Pasadena, California, 7 July 1993.

APPENDIX

Planet or satellite approach trajectories are typically described in aiming plane coordinates referred to as "B-plane" coordinates (see Figure A-1). The B-plane is a plane passing through the planet center and perpendicular to the asymptote of the incoming trajectory (assuming 2 body conic motion). The "B-vector" is a vector in that plane, from the planet center to the piercing-point of the trajectory asymptote. The B-vector specifies where the point of closest approach would be if the target planet had no mass and did not deflect the flight path. Coordinates are defined by three orthogonal unit vectors, S, T, and R with the system origin at the center of the target body. The S vector is parallel to the spacecraft V_{∞} vector (approximately the velocity vector relative to the target body at the time of entry into the target body's gravitational sphere of influence). T is arbitrary, but typically specified to lie in the ecliptic plane (the mean plane of the Earth's orbit), or in a body equatorial plane. Finally, R completes an orthogonal triad with S and T.

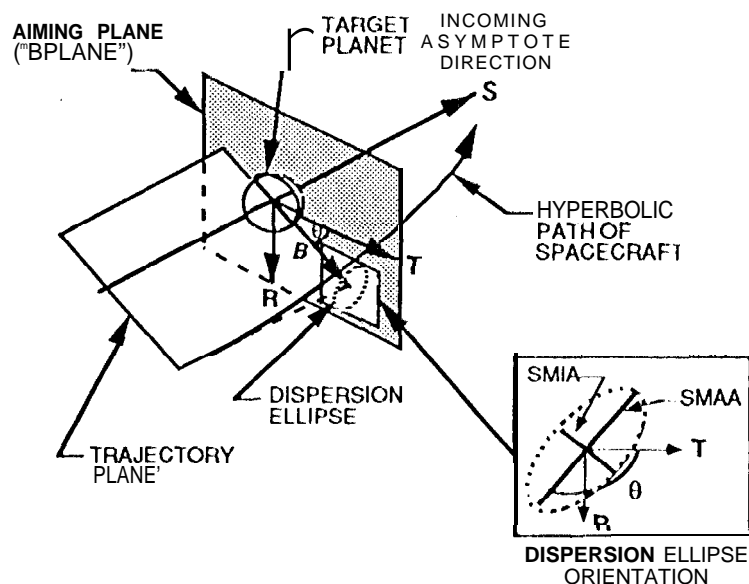


Figure A-1 Aiming Plane Coordinate System Definition

Orbit **determination** errors can be **characterized** by a one-sigma B-plane dispersion ellipse, also shown in Fig. A-1, and the one-sigma uncertainty along the S (or **downtrack**) direction. In Fig. A-1, SMIA and SMAA denote the **semi-minor** and semi-major axes **of** the dispersion ellipse.